

# The influence of chemical composition on initial permeability frequency spectra of cobalt ferrites

V. VILCEANU, M. FEDER<sup>a</sup>, L. BOUTIUC<sup>b</sup>, I. DUMITRU<sup>b</sup>, O. F. CALTUN<sup>b\*</sup>

*S. C. Afero Exim srl, P. O. Box 39-D6, Bucharest, Romania*

<sup>a</sup>*National Institute of Material Physics, P.O. Box MG-7, Bucharest, Romania*

<sup>b</sup>*Faculty of Physics and Carpath Center, Al. I. Cuza University, 700506 Iasi, Romania*

In order to study the influence of the cations substitution on permeability of cobalt ferrites four series of samples with different chemical composition were prepared by conventional ceramic method. The calcined powders and sintered samples were characterized by X-ray diffraction and vibrating samples magnetometer. The microstructure of the samples was analyzed by surface electron microscopy. The initial permeability spectra at room temperature were plotted using the torus standard method. Chemical composition and the microstructure influence the magnetic properties and the initial permeability spectra of the cobalt ferrites samples. Small amount of manganese ions decreases the Curie temperature, increase the initial permeability and saturation magnetization and decreases the coercive magnetic field, thus improving the performances of cobalt ferrites for magnetostrictive sensors applications.

(Received January 27, 2010; accepted June 16, 2010)

*Keywords:* Cobalt ferrites, Cation distribution magnetic properties, Initial permeability

## 1. Introduction

In the last years cobalt ferrites were intensely studied as possible magnetostrictive material to be used in sensor applications. They have the advantages of lower costs, as compared to the metal alloys, and higher restivity hampering the appearance of the eddy currents.

There are parameters strongly influencing the magnetic properties of the ferrites. The deviation from the stoichiometric composition and the substitutions modify the magnetic properties of ferrites [1-4]. The sintering temperature influences the microstructure, the density and porosity consequently the initial permeability value and the permeability spectra [5, 7].

The cobalt ferrites are spinels and their properties depend on composition. The formation of spinelic solid solutions implies the substitution of the bivalent cation with another bivalent one, or a combination of cations to insure the electrical neutrality of the ensemble. The distribution of the substituting ions in tetrahedral or octahedral sites depends on the ionic radius, charge and electronic configuration of the cations [8].

The present study is focused on the influence of the chemical composition and of the microstructure on the magnetic properties of cobalt ferrites and on the initial permeability spectra. Four categories of samples were studied: stoichiometric cobalt ferrite ( $\text{CoFe}_2\text{O}_4$ ) cobalt ferrite with excess of iron ( $\text{Co}_{0.8}\text{Fe}_{2.2}\text{O}_4$ ) cobalt ferrite with manganese substitution ( $\text{CoMn}_{0.2}\text{Fe}_{1.8}\text{O}_4$ ) and cobalt ferrite with silicon substitution ( $\text{Co}_{1.3}\text{Si}_{0.3}\text{Fe}_{1.4}\text{O}_4$ ).

## 2. Experimental

Cobalt ferrite samples with different chemical compositions were synthesized using the high-temperature ceramic method [9-11].

The starting materials all produced by Merck were added in a steel ball mill in appropriate concentrations and mixed for 8 hours in a water solution. After oven drying, the mixtures were calcined and sintered as shown in Table 1. The so calcined material was wet milled without any additive in ball mills for 16 hours.

Using a DRON X-ray  $\text{Cu K}\alpha$  radiation diffraction meter the ferrites powders were investigated. Were identified the phases and calculated the lattice constants.

The row ferrite powders were pressed into ring core (outer diameter, inner diameter and thickness of 17, 11 and 5mm respectively) and cylindrical (diameter of 11mm and height of 5mm) shapes. The green density of the specimens was  $2.8 \pm 0.2 \text{ g}\cdot\text{cm}^{-3}$ . The samples were sintered in air at  $1300^\circ\text{C}$  for 5 hours.

Microstructure analysis on fractured surface of sintered samples was performed using a surface electron microscope.

The magnetic properties were measured by vibration sample magnetometer. From the hysteresis loops was deduced and plotted the maximum magnetization, remanence magnetization and coercive field values.

The initial permeability of cobalt ferrites were measured on torus shaped samples in conformity with the standard procedure IEC 60401 ( $f \leq 10 \text{ kHz}$ ,  $B < 0.25 \text{ mT}$ ,  $T = 250^\circ\text{C}$ ) [12].

Table 1. Cobalt ferrites prepared by conventional ceramic method.

Chemical composition of samples	Starting materials	First calcination	Second calcination	Sintering process
$\text{CoFe}_2\text{O}_4$	$\alpha\text{-Fe}_2\text{O}_3$ Merck(>99% $\text{Fe}_2\text{O}_3$ ) $\text{Co}_3\text{O}_4$ Merck (>99 $\text{Co}_3\text{O}_4$ )	900°C 5h, air	900°C 5h, air	1300°C 5h, air
$\text{Co}_{0.8}\text{Fe}_{2.2}\text{O}_4$	$\alpha\text{-Fe}_2\text{O}_3$ Merck(>99% $\text{Fe}_2\text{O}_3$ ) $\text{Co}_3\text{O}_4$ Merck (>99 $\text{Co}_3\text{O}_4$ )	900°C 5h, air	900°C 5h, air	1300°C 5h, air
$\text{CoMn}_{0.2}\text{Fe}_{1.8}\text{O}_4$	$\alpha\text{-Fe}_2\text{O}_3$ Merck(>99% $\text{Fe}_2\text{O}_3$ ) $\text{Co}_3\text{O}_4$ Merck (>99 $\text{Co}_3\text{O}_4$ ) $\text{MnCO}_3$ Merck(54%MnO)	950°C 5h, air	950°C 5h, air	1300°C 5h, air
$\text{Co}_{1.3}\text{Si}_{0.3}\text{Fe}_{1.4}\text{O}_4$	$\alpha\text{-Fe}_2\text{O}_3$ Merck(>99% $\text{Fe}_2\text{O}_3$ ) $\text{Co}_3\text{O}_4$ Merck (>99 $\text{Co}_3\text{O}_4$ ) $\text{SiO}_2$ p.a.(>99% $\text{SiO}_2$ )	950°C 5h, air	950°C 5h, air	1300°C 5h, air

### 3. Results and discussion

The XRD patterns of the sintered samples are shown in Fig. 1.

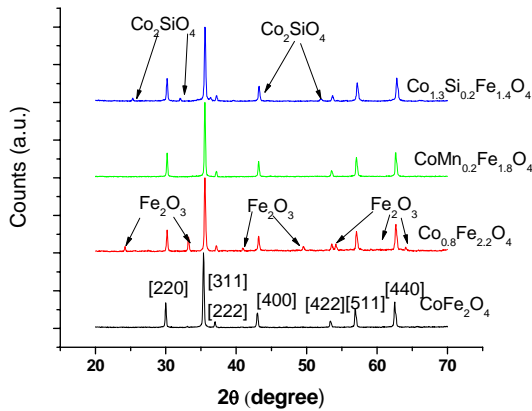


Fig.1. The XRD patterns of sintered samples

Refined X-ray diffraction data show that samples are mainly composed of spinel phase (Table 2) [13]. The studied samples are two-phase system, commonly obtained when using conventional high-temperature technique to get spinel ferrites [8]. The sample  $\text{CoFe}_2\text{O}_4$  has a small concentration of hematite while  $\text{Co}_{0.8}\text{Fe}_{2.2}\text{O}_4$  has larger concentration. No residual phase was observed in the case of  $\text{CoMn}_{0.2}\text{Fe}_{1.8}\text{O}_4$  while in the case of  $\text{Co}_{1.3}\text{Si}_{0.3}\text{Fe}_{1.4}\text{O}_4$  there is a small amount of cobalt silicate. The lattice parameters of studied samples are smaller than theoretical value for  $\text{CoFe}_2\text{O}_4$  of  $8.38\text{\AA}$  [8], with the exception of  $\text{CoMn}_{0.2}\text{Fe}_{1.8}\text{O}_4$  sample.

The properties of the ferrite cores are determined essentially by their microstructures shown in Fig. 2. The sample  $\text{CoFe}_2\text{O}_4$  displays a microstructure with relatively uniform grains, with open porosity including big hematite particles. The sample  $\text{Co}_{0.8}\text{Fe}_{2.2}\text{O}_4$  displays a microstructure with relatively fine grains and a narrow dispersion of sizes but the big hematite grains are more frequent. The microstructure of  $\text{CoFe}_{1.8}\text{Mn}_{0.2}\text{O}_4$  sample is

more uniform and the grains distribution is narrow. The sample  $\text{Co}_{1.3}\text{Si}_{0.3}\text{Fe}_{1.4}\text{O}_4$  displays an abnormal grain growth type microstructure including both giant and very small grains, with a few pores located inside the grains and with cobalt silicate segregated at the boundaries [12].

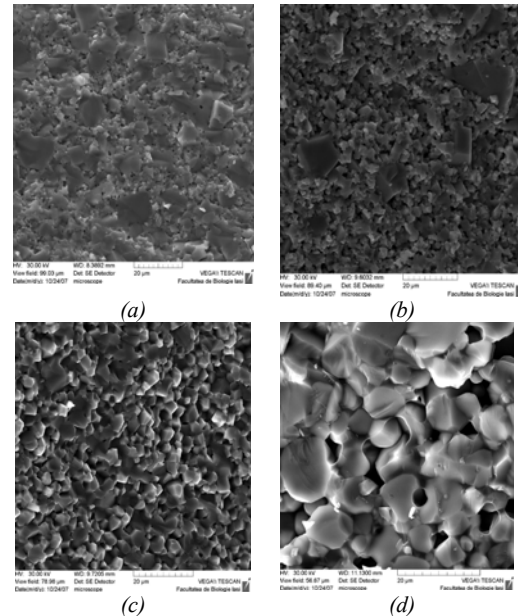


Fig. 2. SEM microphotographs of bodies sintered for 5 hours at  $1300^\circ\text{C}$ , in air: a)  $\text{CoFe}_2\text{O}_4$ ; b)  $\text{Co}_{0.8}\text{Fe}_{2.2}\text{O}_4$ ; c)  $\text{CoFe}_{1.8}\text{Mn}_{0.2}\text{O}_4$  d)  $\text{Co}_{1.3}\text{Si}_{0.3}\text{Fe}_{1.4}\text{O}_4$

The Mössbauer suggested the presence of the iron in the  $\text{Fe}^{3+}$  oxidation state analysis according to the isomer shift values. The iron excess in sample  $\text{Co}_{0.8}\text{Fe}_{2.2}\text{O}_4$  is preferentially found in the octahedral positions of the spinel lattice. The manganese ions preferentially substitute iron in the octahedral positions because  $\text{Fe}^{3+}$  has higher preference for the tetrahedral positions, as compared to the  $\text{Co}^{2+}$  and  $\text{Mn}^{3+}$  cations. The silicon ions preferentially substitute  $\text{Fe}^{3+}$  from the octahedral positions [14,15].

Table 2. Data from XRD patterns of cobalt ferrites samples.

Sample	Unit cell length $a_0$ (Å)	$d_{RX}$ (g/cm <sup>3</sup> )	Phases (%)
CoFe <sub>2</sub> O <sub>4</sub>	8.3776	5.30	97.80% spinel, 2.20% hematite
Co <sub>0.8</sub> Fe <sub>2.2</sub> O <sub>4+δ</sub>	8.3825	5.28	75.60% spinel, 24.40% hematite
CoFe <sub>1.8</sub> Mn <sub>0.2</sub> O <sub>4</sub>	8.3888	5.28	100 spinel
Co <sub>1.3</sub> Si <sub>0.3</sub> Fe <sub>1.4</sub> O <sub>4</sub>	8.3562	5.17	95,50% spinel 4,50% cobalt silicate

Table 3. Physical and magnetic properties of samples sintered in various conditions.

Sintering Parameters	Sample	d (g/cm <sup>3</sup> )	P (%)	M <sub>max</sub> (emu/g)	M <sub>r</sub> (emu/g)	H <sub>c</sub> (Oe)	T <sub>c</sub> (°C)	μ <sub>i</sub> 20°C, 10kHz
1300°C 5h	CoFe <sub>2</sub> O <sub>4</sub>	4.74	10.60	59	13	504	520	18
	Co <sub>0.8</sub> Fe <sub>2.2</sub> O <sub>4</sub>	4.50	14.77	70	15	474	530	21
	CoMn <sub>0.2</sub> Fe <sub>1.8</sub> O <sub>4</sub>	4.82	8.71	100	9	126	450	26
	Co <sub>1.3</sub> Si <sub>0.3</sub> Fe <sub>1.4</sub> O <sub>4</sub>	4.53	12.38	51	4	81	505	23

The vibration sample magnetometer measurements are shown in Fig. 3 and the data are summarized in Table 3.

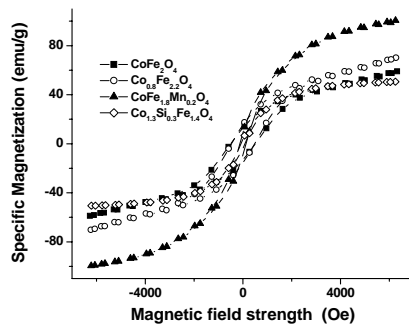


Fig. 3. The hysteresis loops of sintered samples.

Comparatively with CoFe<sub>2</sub>O<sub>4</sub> sample, silicon substituted cobalt ferrite shows a small decrease of the magnetization proving the silicon ions entrance in the spinel lattice. The significant decrease of the coercive field stands for abnormal microstructure of the Co<sub>1.3</sub>Si<sub>0.3</sub>Fe<sub>1.4</sub>O<sub>4</sub> sample. The large particles and the interparticles bridges entail the decrease of the coercive field. Sample CoFe<sub>1.8</sub>Mn<sub>0.2</sub>O<sub>4</sub> has the highest value of the specific magnetization and highest initial permeability value. Characterized by a narrowed uniform grain size distribution this ferrite is recommended for sensors applications.

Rich iron cobalt ferrite show the highest Curie temperature and a higher specific magnetization comparatively with the stoichiometric cobalt ferrite justified by the iron cations excess.

Based on analysis of experimental results from Table 4 it can be concluded that CoFe<sub>2</sub>O<sub>4</sub> and CoFe<sub>1.8</sub>Mn<sub>0.2</sub>O<sub>4</sub> samples show adequate magnetic and magnetostrictive properties useful for applications. The dependence of the initial permeability spectra on the temperature of the sintered samples are shown in Fig. 4.

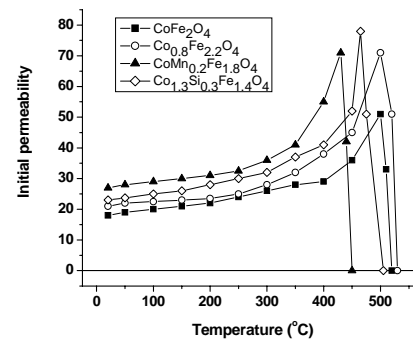


Fig. 4. The initial permeability spectra of the sintered samples vs. temperature.

The initial magnetic permeability is a very microstructure-sensitive property. The shape of the experimental permeability spectra for our samples is a normal one. As observed in most of the magnetic materials the initial permeability  $\mu_i$  increases with temperature up to Curie temperature  $T_c$ . According to the reversible displacement of domain walls, the initial permeability  $\mu_i$  can be expressed as [16]

$$\mu_i \propto \frac{M_s^2}{K_1}$$

where  $M_s$  and  $K_1$  are the saturation magnetization and crystalline magneto-anisotropy constant, respectively. The thermal variations of  $\mu_i$  should therefore correspond to the thermal variations of  $M_s^2 / K_1$ . Because the saturation magnetization of ferrites decreases slowly with temperature, while their anisotropy constant decreases much more rapidly the initial permeability shows therefore an increase with temperature. At the Curie point, the initial permeability drops from its maximum value to the value corresponding to the paramagnetic phase. Ohta [17] have observed that the initial permeability is maximum at a temperature where the anisotropy constant changes its sign.

We used the temperature dependence of the initial permeability as a method for Curie temperature determination. The Table 3 summarizes the obtained values for Curie temperature and initial permeability at low temperature. It is observed that the measured values of the initial permeability are proportional with the saturation magnetization of the samples, the low values of the initial permeability for all samples are explained by the high values of the coercive field and anisotropy constant.

The abrupt drop of the initial permeability at the Curie point, from its maximum value to the value corresponding to the paramagnetic phase, proves the chemical homogeneity of our samples [18].

#### 4. Conclusions

The cobalt ferrites studied in this paper demonstrates the sensitivity of the magnetic properties to the chemical composition and to the parameters of the sintering process. A small deviation of the chemical composition from the stoichiometry influences the microstructure and the magnetic properties. A small amount of iron ions in excess increases the Curie temperature unsought for the cobalt ferrite material for magnetostrictive sensors. A small amount of silicon ions promotes the grain growth but by sintering the samples at high temperature the growing process is an abnormal one and the properties of silicon substituted cobalt ferrites are affected. The manganese substitution of the iron ions improves the microstructure of the cobalt ferrites for sensors applications. The Curie temperature is strongly decreased by the entrance of the manganese ions in the spinel lattice replacing the iron cations. In the same time the specific magnetization of the manganese substituted cobalt ferrites significantly increases while the coercive field decreases.

Briefly, the  $\text{CoFe}_{1.8}\text{Mn}_{0.2}\text{O}_4$  ferrite has the best ensemble of magnetic properties useful for applications as sensors.

#### Acknowledgements

These results were obtained in the PNII 12-093 HIF1, financed by Romanian Ministry of Education and Research.

#### References

- [1] J. A. Paulsen, C. C. H. Lo, J. E. Snyder, A. P. Ring, L. L. Jones, D.C. Jiles, *IEEE Trans. Magn.* **39**, 3316 (2003).
- [2] D. B. Shekhar, P. A. Joy, *J. Appl. Phys.* **99**, 073901 (2006).
- [3] O. F. Caltun, H. Chiriac, N. Lupu, I. Dumitru, B. Parvatheeswara Rao, *J. Optoelectron. Adv. Mater.* **9**(4), 1158 (2007).
- [4] G. S. N Rao, S. Ananda Kumar, K. H Rao, B. Parvatheeswara Rao, A. Gupta, O. Caltun, I. Dumitru, K. CheolGi, *Proceedings of the 2nd IEEE International Conference on Nano/Micro Engineered and Molecular Systems*, January 16 - 19, 2007, Bangkok, Thailand, 1186 (2007).
- [5] T. Nakamura, *JMMM* **168**, 285 (1997).
- [6] O. F. Caltun, L. Spinu, Al. Stancu, L. D. Thung, W. Zhou, *JMMM* **160-162** Part 1, 242 (2002).
- [7] A. Paduraru, M. Feder, O. F. Caltun, *J. Optoelectron. Adv. Mater.* **5**(4), 945 (2003).
- [8] A. Goldman, *Modern Ferrite Technology*, 2nd ed., 2006, Springer New York.
- [9] K. Kriebel, T. Schaeffer, J. A. Paulsen, A. P. Ring, C. C. H. Lo, J. E. Snyder, *J. Appl. Phys.* **97**, 10F101 (2005).
- [10] S. J. Lee, C. C. H. Lo, P. N. Matlage, S. H. Song, Y. Melikhov, J. E. Snyder, D. C. Jiles, *J. Appl. Phys.* **102**, 073910 (2007).
- [11] J. A. Paulsen, A. P. Ring, C. C. H. Lo, J. E. Snyder, D. C. Jiles, *J. Appl. Phys.* **97**, 044502 (2005).
- [12] *EPCOS – Ferrites and Accessories. Data Book 2007.*
- [13] G. Winkler, *Magnetic Properties of Materials*, McGraw-Hill Book Comp., N.Y. 1971.
- [14] Sang Won Lee, Chul Sung Kim, *JMMM* **303**, e315 (2006).
- [15] Y. Ahn, E. J. Choi, H.N. Ok, S. Kim, *Mat. Lett.* **50**(1) 47 (2001).
- [16] S. Chikazumi, *Physics of Magnetism*, John Wiley & Sons, Inc., New York, 1964.
- [17] K. Ohta, *J. Phys. Soc. Jpn.* **18**, 685 (1963).
- [18] D. Arcos, R. Valenzuela, M. Vazquez, M. Vallet-Regi, *Journal of Solid State Chemistry* **141**, 10 (1998).

\*Corresponding author: caltun@uaic.ro